ELSEVIER

Biophysical Chemistry 110 (2004) 73–81

Biophysical Chemistry

www.elsevier.com/locate/bpc

Linkage of proton binding to the thermal dissociation of triple helix complex

Luigi Petraccone[a], Eva Erra[b], Carlo Andrea Mattia[a], Vito Fedullo[c], Guido Barone[b], Concetta Giancola[b,*]

[a] *Dipartimento di Scienze Farmaceutiche, Via Ponte Don Melillo, 84084, Fisciano (SA), Italy*
[b] *Dipartimento di Chimica, Università 'Federico II' di Napoli, Via Cintia 4, 80126, Napoli, Italy*
[c] *Dipartimento di Matematica e Informatica, Via S. Allende, 84081, Baronissi (Sa), Italy*

Received 26 September 2003; received in revised form 5 January 2004; accepted 5 January 2004
Available online 5 May 2004

Abstract

The effects of cytosine protonation on the thermodynamic properties of parallel pyrimidine motif DNA triplex were investigated and characterized by different techniques, such as circular dichroism (CD), ultraviolet spectroscopy (UV) and differential scanning calorimetry (DSC). A thermodynamic model was developed which, by linking the cytosine ionization equilibrium to the dissociation process of the triplex, is able to rationalize the experimental data and to reproduce the pH dependence of the free energy, enthalpy and entropy changes associated with the triplex formation. The results are useful to systematically introduce the effect of pH in a more general model able to predict the stability of DNA triplexes on the basis of the sequence alone.

Keywords: DNA triple helix; Cytosine protonation; Thermodynamic stability; Differential scanning calorimetry; Circular dichroism

1. Introduction

The triple helix structure, because of possible applications in biotechnology, diagnostics and therapeutics, has attracted considerable attention [1–3]. Numerous attempts have been made to use oligonucleotides, particularly triple-helix-forming oligonucleotides as tools for exploring DNA structure and for creating methods for regulation of gene expression and genome analysis. Triple helices can be subdivided into intermolecular and intramolecular complexes and have parallel and antiparallel structures according to the composition and orientation of the third strand. The base composition of the third strand can be purine or pyrimidine rich. A homopyrimidine third strand binds parallel to the purine strand of the target duplex forming T−A·T and C−G·C^+ triplets via Hoogsteen hydrogen bonding [4–6], whereas a purine third strand binds in an anti-parallel orientation forming T−A·A and C−G·G base triplets via reverse Hoogsteen hydrogen bonds [7]. In the parallel motif triplexes, the requirement for protonation of the cytosine

* Corresponding author. Tel.: +39-081-674266; fax: +39-081-674090.
E-mail address: giancola@chemistry.unina.it (C. Giancola).

0301-4622/$ - see front matter © 2004 Elsevier B.V. All rights reserved.
doi:10.1016/j.bpc.2004.01.004

bases results in a dependence on pH of the three-stranded complex's stability [8–10]. Surprisingly, a complete thermodynamic characterization of a triplex helix stability as a function of pH has been lacking. Typically, only melting temperatures are reported on changing the pH and the other thermodynamic quantities (enthalpy, entropy, free energy) associated with the transition are usually reported at only one value of the pH. Consequently, the protonation effect on the thermodynamic parameters has not been clearly understood. The evaluation of these parameters on changing the pH should inform us about the mechanism of triplex formation. Thus, it is important to investigate the details of the thermodynamic properties for the triplex transition.

It is known that the sensitivity of triplex stability to pH is dependent on the relative number of cytosines in the third strand, as well as their positions relative to each other and relative to the ends of the third strand [11,12]. Since the pK_a of the cytosine in single-stranded DNA is approximately 4.5, third strand dissociation at pH above this value is accompanied by release of protons from the protonated cytosine residues [13]. The apparent pK_a of third strand association is typically much higher than the intrinsic pK_a of the cytosine indicating that the protonation event and association of the third strand to the target duplex are coupled in some way and the local environment of the cytosine residue shifts the intrinsic pK_a to a value higher than the pK_a of the third strand [12].

NMR studies with isotope-labeled triple helices evaluated the intrinsic pK_a of the cytosines at specific sites within triplex structure [12,14,15]. These studies showed that, in some cases, the deprotonation of cytosine residues can occur before the third strand dissociation. This finding suggests that third strands containing mixtures of C and T bases should be able to form triplexes also at high pH because unprotonated cytosine residues can interact with GC base-pairs to form triplets of finite stability with a single H-bond. Therefore the triplex may exist in various states of protonation in dependence on pH conditions and all these different states may be characterized by a specific enthalpy, entropy and free energy levels, which can affect the thermodynamics of triplex formation. In this hypothesis, to perform a complete thermodynamic characterization of single strand binding to target duplex on changing the pH, it is important to relate protonation equilibria within the triplex to the thermodynamics of triplex formation.

In this paper, it was studied the thermodynamic properties for the triplex formation process between a target homopurine–homopirimidinic duplex $^{5'}$AGAGAGAGAGAGAGAG$^{3'}$.$^{5'}$CTCTCTCTCTC-CTCTCTCTCTCTCTCT$^{3'}$, and a homopyrimidine cytosine-rich single strand, $^{5'}$TCTCTCTCTCTCT-CTC$^{3'}$. The thermodynamic parameters were obtained by DSC, UV and CD experiments and it developed a thermodynamic model, which, by linking the cytosine ionization equilibrium to the dissociation process of the triplex, is able to reproduce the pH dependence of the free energy, enthalpy and entropy changes associated with the triplex formation.

2. Materials and methods

2.1. Oligonucleotides

The oligonucleotides investigated in this study are:

$^{5'}$CTCTCTCTCTCTCTCT$^{3'}$;
$^{3'}$GAGAGAGAGAGAGAGA$^{5'}$;
$^{3'}$CTCTCTCTCTCTCTCT$^{5'}$.

These oligonucleotides were synthesized on an automated DNA synthesizer following standard phosphoramidite procedures [16–18]. The triplex was formed by mixing stoichiometric amounts of oligonucleotides in the appropriate buffer and heating the solution to 90 °C for 5 min. The solution was slowly cooled to room temperature, then equilibrated for one day at 4 °C. The buffer used was 140 mM KCl, 5 mM NaH_2PO_4, 5 mM $MgCl_2$. Potassium chloride (Sigma), monosodium phosphate (Sigma) and magnesium chloride (Carlo Erba) were used as obtained from commercial suppliers. Each of the solutions was adjusted to desired pH values with 1 M HCl or 1 M NaOH. The pH of solutions was measured using a Radiometer pHmeter model PHM 93 at 25 °C. The concentration of oligonucleotide solutions were determined spectrophotometrically at 260 nm, using the following extinction coefficients calculated by a nearest neighbor model [19], 122000 M^{-1} cm^{-1} for $^{5'}(TC)_8^{3'}$, 123000 M^{-1} cm^{-1} for $^{5'}(CT)_8^{3'}$ and 188000 M^{-1} cm^{-1} for $^{5'}(AG)_8^{3'}$.

2.2. Circular dichroism

CD spectra were obtained on a JASCO 715 circular dichroism spectrophotometer at 5 °C in a 0.1 cm pathlength cuvette. The wavelength was varied from 200 to 340 nm at 5 nm min^{-1}. CD spectra were recorded with a response of 16 s, at 2.0 nm bandwidth and normalized by subtraction of the background scan with buffer. The titrations were accomplished by addition of microliter amounts of 1 M HCl to the solution containing the triplex. The pH of solutions was monitored by directly inserting a pH electrode designed for microsamples (Hamilton Glass) into cuvettes containing the sample. The molar ellipticity was calculated from the equation $[\vartheta]=100\vartheta/cl$ where ϑ is the relative intensity, c the concentration of triplex and l is the path length of the cell in centimetres. Each spectrum is an average of at least three scans. The sigmoidal curve was obtained using the Boltzman fit of Origin program. Temperature was kept constant with a thermoelectrically controlled cell holder (JASCO PTC-348).

2.3. Ultraviolet spectroscopy

Absorbance vs. wavelength curves were measured using a Jasco V-530 UV/VIS spectrophotometer at 25 °C in a 1 cm pathlength cuvette. The wavelength was varied from 260 to 340 nm at 5 nm min^{-1}. pH titrations were accomplished by addition of microliter amounts of 1 M HCl to the solution containing the $^{3'}$CTCTCTCTCTCTCTCT$^{5'}$. For pH<5.8, where the phosphate is not an appropriate buffer, the pH of solutions was monitored by directly inserting a pH electrode designed for microsamples (Hamilton Glass) into cuvettes containing 1.5 ml of sample.

Temperature was kept constant with a thermoelectrically controlled cell holder (JASCO PTC-348).

2.4. Differential scanning calorimetry

DSC measurements were performed on a second generation Setaram Micro-DSC at scan rate of 0.5 °C/min. The calorimetric unit was interfaced to an IBM PC computer for automatic data collection and analysis using the software previously described [20]. The apparent molar heat capacity vs. temperature profiles were obtained by subtracting buffer vs. buffer curves from the sample vs. buffer curves. The data were normalized with regard to the concentration, sample volume and scan rate. The performance of the instrument was calibrated periodically with an electrical pulse. The excess heat capacity function $\langle \Delta C_P \rangle$ was obtained after baseline subtraction, assuming that the baseline is given by the linear temperature dependence of the native state heat capacity [21]. The reversibility of the thermal processes was verified by checking the reproducibility of the calorimetric trace in a second heating of the samples immediately after cooling from the first scan. The process enthalpies, $\Delta H^\circ(T_m)$, were obtained by integrating the area under the heat capacity vs. temperature curves. T_m is the temperature corresponding to the maximum of each DSC peak. The process entropies, $\Delta S^\circ(T_m)$, were determined integrating the curve obtained by dividing the heat capacity curve by the absolute temperature, i.e. $\Delta S^\circ = \int(\langle \Delta C_p \rangle / T)\mathrm{d}T$. The free energy change was calculated at each pH value using the relationship $\Delta G^\circ = \Delta H^\circ - T\Delta S^\circ$, assuming a negligible difference in heat capacity between the initial and final states. Indeed, no significant ΔC_P was observed as already found in DSC studies on triplex dissociation process by different authors [22,23]. The buffer used was 140 mM KCl, 5 mM NaH_2PO_4 and 5 mM $MgCl_2$. Experiments were performed in the pH range of 5.5–7.2. The $\delta[H^+]/\delta T$ is assumed to be negligible because the phosphate buffer has a low ionization enthalpy.

The errors in T_m do not exceed 0.2 °C, the errors for $\Delta H^\circ(T_m)$ and $\Delta S^\circ(T_m)$ are the standard deviations of the means from the multiple measurements.

3. Results

3.1. Thermodynamic parameters of triplex formation

The thermodynamic stability of the triplex was studied in the pH range of 5.5–7.2, keeping the triplex concentration constant at 4.4×10^{-4} M. The thermal dissociation of the third strand is a reversible, not kinetically limited process, in fact, repeated heating and cooling of DSC samples at different scan rate produced superimposable thermograms at each investigated pH value. It was not possible to evaluate the thermodynamic parameters at pH values higher than 7.2 because the triplex begins to melt at temperature

not experimentally accessible. The pH values lower than 5.5 could not be tested because the extensive protonation of the hydrogen-bonding groups of the duplex bases disrupts the whole hydrogen-bonded structure and the DNA aggregates in the solution [24].

The characteristic calorimetric profile for the triplex at pH 7.2 is shown in Fig. 1. The first low-temperature transition is attributable to the release of the third strand from the target duplex and the second transition at higher temperature is relative to the dissociation of the double helix in the two single strands. The overall process can be represented according to the scheme:

$$ABC \leftrightarrows A + BC \quad (I)$$

$$BC \leftrightarrows B + C \quad (II)$$

where ABC indicates the triplex, BC the target duplex, A indicates the third strand. The first process (I) is strongly dependent on the pH values and, at low pH values, a previously described deconvolution procedure was used to extract thermodynamic quantities by calorimetric profiles because the two transitions are not well separated [18]. The second process (II) is independent of pH in the range 5.7–7.2 whereas at pH 5.5 an increasing of the duplex thermal stability is observed, according to the protonation of the duplex bases cited above [24]. Table 1 summarizes the thermodynamic parameters for the dissociation process of the third strand from the target duplex in the pH range of 5.5–7.2. Thermodynamic parameters at pH values of 7.2, 6.8, 6.0 and 5.5 were previously obtained [18]. Inspection of the table reveals that all the thermodynamic quantities decrease with increasing the pH. Particularly, on increasing the pH from 5.5 to 7.2, the T_m decreases of approximately 34 °C and the enthalpy and entropy changes decrease of approximately 130 kJ mol^{-1} and 0.3 kJ mol^{-1} K^{-1}, respectively. Hence, increasing pH, the enthalpic term becomes more favorable to the dissociation process whereas the entropy term becomes less favorable.

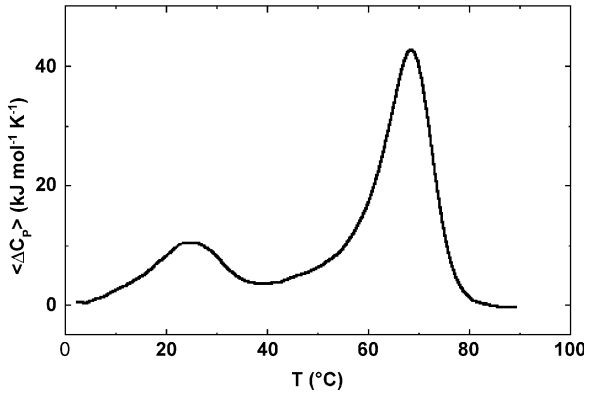

Fig. 1. Differential scanning calorimetric curve for the triplex at pH 7.2. The triplex concentration was 4.4×10^{-4} M.

Table 1
Thermodynamic parameters for ABC⇆A+BC transition[a]

pH	T_m (°C)	$\Delta H°$ (T_m) (kJ mol^{-1})	$\Delta S°$ (T_m) (kJ mol^{-1} K^{-1})	$\Delta G°$ (298 K) (kJ mol^{-1})
7.2	25.2±0.2	130±13	0.48±0.06	−13.0±0.1
7.0	31.4±0.2	150±12	0.54±0.05	−10.9±0.3
6.8	34.0±0.2	190±10	0.64±0.04	−0.7±0.3
6.6	48.0±0.2	215±8	0.70±0.04	6.4±0.6
6.4	52.0±0.2	230±9	0.73±0.05	12.5±0.8
6.0	58.5±0.2	255±7	0.78±0.02	22.6±0.7
5.7	59.0±0.2	262±9	0.79±0.02	26.6±0.9
5.5	59.0±0.2	256±7	0.79±0.02	20.6±0.7

[a]For BC⇆B+C transition the thermodynamic parameters at pH 7.2-5.7 are: T_m=69.0 °C, $\Delta H°(T_m)$=480±16 kJ mol^{-1} and $\Delta S°(T_m)$=1.40±0.05 kJ mol^{-1} K^{-1}.

At pH 5.5 for the same transition the thermodynamic parameters are: T_m=77.0 °C, $\Delta H°(T_m)$=480±16 kJ mol^{-1} and $\Delta S°(T_m)$=1.37±0.05 kJ mol^{-1} K^{-1}.

3.2. Circular dichroism

Fig. 2 shows the CD spectra at pH 6.4 of triplex, duplex and single strands, respectively. The CD spectrum of the triplex is characterized by a large positive band at 276 nm and a negative band at 215 nm. The last one is consistent with the existence of triple stranded DNA [25]. Circular dichroism spectra of the triplex as a function of pH were performed. The triplex concentration was 1.3×10^{-5} M. As the pH is increased, the negative band at 215 nm is reduced in magnitude and shifted to lower wavelength, while the positive band at 276 nm is slightly increased in magnitude and shifted to lower wavelength (data not shown). These findings are consistent with a pH-induced transition relative to dissociation of the third strand from the target double helix. Fig. 3 shows the pH dependence of molar ellipticity at 215 nm: this

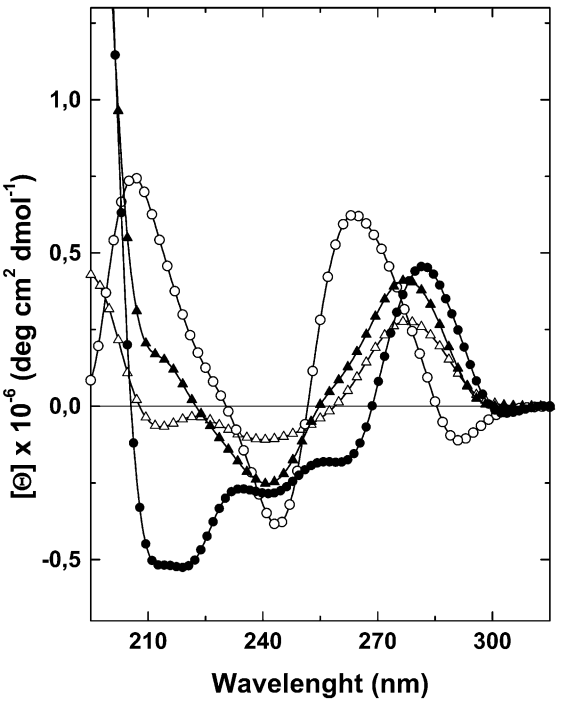

Fig. 2. Circular dichroism spectra of the triplex (●), duplex (▲), $^{3'}(GA)_8^{5'}$ (○), $^{5'}(CT)_8^{3'}$ and $^{3'}(CT)_8^{5'}$ (△) at pH 6.4. All the spectra were recorded at 5 °C.

plot has a sigmoidal behavior with an inflection point at pH 7.0.

3.3. Ultraviolet spectroscopy

In order to evaluate a pK_a value for the cytosine residues in the isolated third strand a UV titration experiment was performed. The single strand concentration was 5.0×10^{-6} M. Fig. 4 shows changes of the absorbance at 290 nm vs. pH at 25 °C. This plot has a sigmoidal behavior and a semiprotonation point of 4.5 was observed. This value is close to the pK_a value of the free cytosine [26].

3.4. Thermodynamic model

To gain more insight into triplex protonation and its influence on thermodynamic parameters associated with triplex to duplex transition a thermodynamic model was developed. This model, by linking the cytosine ionization equilibrium to the dissociation process of the triplex, is able to rationalize the experimental data and provide a possible explanation of the pH dependence of the thermodynamics of cytosine-rich triplexes formation. The key point of the model is that the oligopyrimidine third strand may exist in different states of protonation not only in the free state but also in the triplex state. The model involves the coupling between the ionization of cytosine residues inside and outside the triplex structure and the thermal dissociation of the third strand. All the cytosine residues are considered identical and non-interacting, with different ionization constants in the triplex and in the free third strand. This hypothesis is reinforced by the observation that, in the third strand utilized, except for the cytosine at the 5′ -end, the cytosine residues have the same local environment constituted by two thymidine residues.

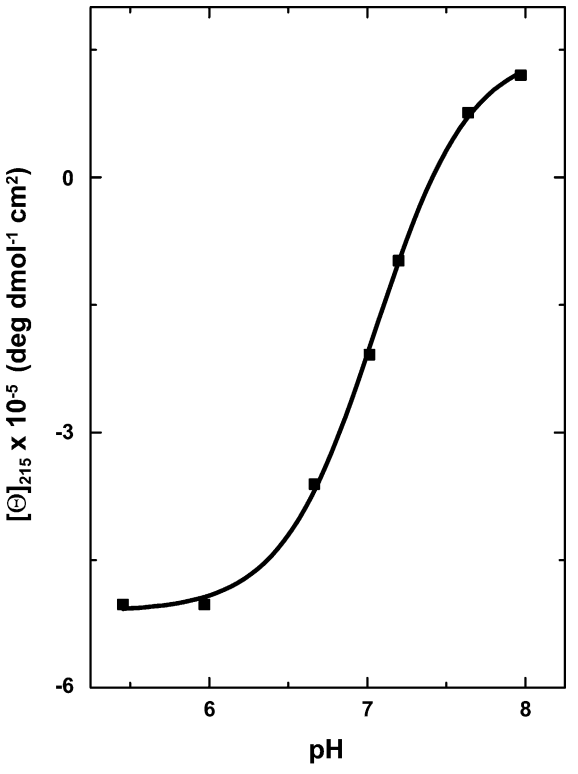

Fig. 3. Molar ellipticity at 215 nm of the triplex as a function of pH. The triplex concentration was 1.3×10^{-5} M.

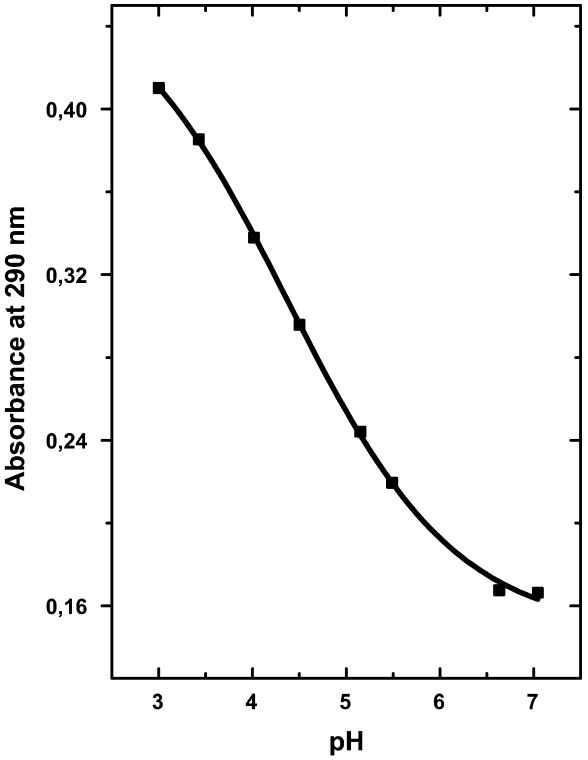

Fig. 4. Absorbance at 290 nm of the $^{3'}(CT)_8^{5'}$ as a function of pH. The single strand concentration was 5.0×10^{-6} M.

The linkage of proton binding to the thermal dissociation of the homopyrimidine third strand can be described by the following equilibria:

$$\begin{array}{ccc} & \overset{K_0}{} & \\ TH_8 & \leftrightarrows & D + SH_8 \\ {\scriptstyle K_a^T}\downarrow\uparrow & \overset{K_1}{} & \downarrow\uparrow\ {\scriptstyle K_a^S} \\ TH_7 & \leftrightarrows & D + SH_7 \\ \downarrow\uparrow & \overset{K_2}{} & \downarrow\uparrow \\ TH_6 & \leftrightarrows & D + SH_6 \\ \downarrow\uparrow & & \downarrow\uparrow \\ \ldots\ldots & \leftrightarrows & \ldots\ldots\ldots\ldots \\ \ldots\ldots & \leftrightarrows & \ldots\ldots\ldots\ldots \\ \downarrow\uparrow & \overset{K_8}{} & \downarrow\uparrow \\ T & \leftrightarrows & D + S \end{array}$$

where TH_i represent the different protonation states of triplex such as those with different degree of protonation of the cytosines, SH_i indicate the corresponding protonation states for the free third strand and D denotes the target duplex. K_i indicates the equilibrium dissociation constant for the ith protonation state of the triplex. K_a^S and K_a^T are the protonation constants for the cytosine residues of the third strand in the free state and in the triplex, respectively. To completely characterize the proposed model, the three independent parameters K_0, K_a^T and K_a^S must be evaluated. Indeed, all other equilibrium constants (K_1, K_2, …, K_8) can be expressed in terms of these independent parameters.

The apparent dissociation constant K(app) for the triplex is given by:

$$K_{\text{app}} = \frac{[\text{D}]([\text{SH}_8] + [\text{SH}_7] + \ldots\ldots + [\text{S}])}{[\text{TH}_8] + [\text{TH}_7] + \ldots\ldots [\text{T}]} \tag{1}$$

In the hypothesis of non-interacting and identical cytosines, the expression for K(app) becomes:

$$K_{\text{app}} = \frac{[\text{D}][\text{SH}_8]}{[\text{TH}_8]} \frac{\left(1 + \frac{K_a^S}{[H^+]}\right)^8}{\left(1 + \frac{K_a^T}{[H^+]}\right)^8} = K_0 \frac{\left(K_a^S + [H^+]\right)^8}{\left(K_a^T + [H^+]\right)^8} \tag{2}$$

where K_0 is the constant for the dissociation process of the completely protonated third strand from the target duplex.

The standard free energy change for the third strand dissociation from the double helix can be obtained applying a fundamental relation of equilibrium thermodynamics:

$$\begin{aligned} \Delta G^\circ(\text{pH}) &= -RT\ln K_0 - 8RT\ln\left(\frac{K_a^S + [H^+]}{K_a^T + [H^+]}\right) \\ &= \Delta_0 G + \Delta\Delta G(\text{pH}) \end{aligned} \tag{3}$$

where the first term $\Delta_0 G$ represents the free energy change in absence of deprotonation events. The second term, pH-dependent, represents the contribution to the free energy change due to the protonation/deprotonation of the third strand cytosines. The values of ΔG°(pH) at 298 K were calculated using the value of $K_a^S=10^{-4.5}$, relative to the cytosine residue in the free third strand. It was experimentally derived by titration curve (Fig. 4). For the pK_a^T, Wilson et al. determined pK_a values in the range 7.0–7.5 using a thermodynamically rigorous method [27]. The best

agreement between the calculated and the experimental values was obtained for the pK_a^T=7.0 and $\Delta_0 G$=91.4 kJ mol^{-1}.

In order to clarify the origin of free energy dependence on pH, the enthalpic and entropic contributions to the ΔG° were calculated. Starting from Eq. (3) and applying fundamental relations of equilibrium thermodynamics, it is possible to obtain for the ΔH°(pH) and ΔS°(pH) the following expressions:

$$\Delta H^\circ(\mathrm{pH}) = \Delta_0 H + \frac{8K_a^S \Delta H_a^S}{K_a^S + [H^+]} - \frac{8K_a^T \Delta H_a^T}{K_a^T + [H^+]} \quad (4)$$

$$\Delta S^\circ(\mathrm{pH}) = \Delta_0 S + 8R\ln\left(\frac{K_a^S + [H^+]}{K_a^T + [H^+]}\right) + \frac{8}{T} \times \left[\left(\frac{K_a^S \Delta H_a^S}{K_a^S + [H^+]}\right) - \frac{\Delta H_a^T K_a^T}{K_a^T + [H^+]}\right] \quad (5)$$

where $\Delta_0 H$ and $\Delta_0 S$ represent the enthalpic and entropic contributions to the $\Delta_0 G$, ΔH_a^T and ΔH_a^S represent the enthalpy change for the deprotonation process in the triplex state and in the free third strand, respectively. The value of ΔH_a^S was taken equal to the enthalpy of deprotonation of the free cytosine nucleotide, reported to be 17.6 kJ mol^{-1} [28]. The ΔH_a^T value represents the enthalpy difference between the protonated and the unprotonated cytosine in the triplex state and it is the enthalpic change for the reaction TAT/CGC$^+$/TAT⇆TAT/CGC/TAT+H$^+$. This enthalpy value is the sum of three contributions: the enthalpy of deprotonation of free cytosine, cited above [28], the enthalpy of one hydrogen bond (one hydrogen bond is lost after deprotonation) reported to be 7.5 kJ/mol [29], and the enthalpy of interaction between the proton charge and the π-electrons of the adjacent TAT triplets. The last contribution should be equal to the difference between the stacking energy of the TAT/CGC$^+$ and the TAT/CGC triplets, it can be negligible [30]. Consequently, it is possible to assign for the deprotonation process of one cytosine inside the triplex, an enthalpy change of ca. 25 kJ/mol. Introducing K_a^T, K_a^S, ΔH_a^S and ΔH_a^T in the relations (4–5), the values of $\Delta_0 H$ and $\Delta_0 S$ can be estimated by fitting the experimental data. The obtained values are: $\Delta_0 H$=145 kJ mol^{-1} and $\Delta_0 S$=0.18 kJ mol^{-1} K^{-1}.

In Fig. 5 are shown the plots of ΔG°, ΔH°, and $-T\Delta S^\circ$ vs. pH at 298 K obtained by means of Eqs. (3)–(5). The plot of ΔG° at 298 K has a sigmoidal behavior with two plateaus, one at pH<4 and another one at pH>8. The plateaus represent the regions where no ionization events occur before and after the triplex dissociation. Moreover, the stability of triplex monotonically decreases on increasing pH. The plots of ΔH° and $-T\Delta S^\circ$ show opposite behavior. There is a good agreement between the experimental points and the theoretical curves in the range of pH experimentally investigated, except for the point at pH 5.5. The deviation from the model at this pH is due to protonation of others group, in addition to the cytosines protonation of the third strand [24].

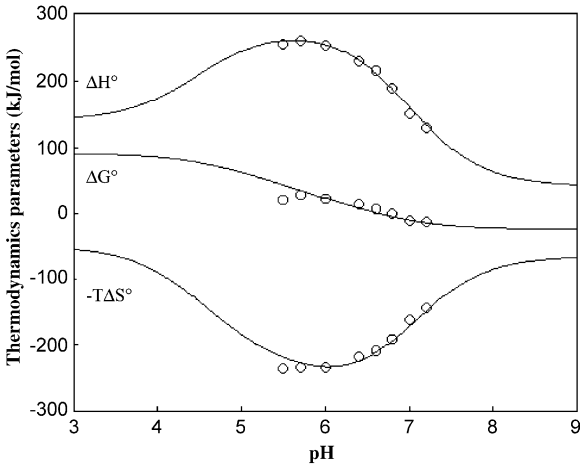

Fig. 5. pH dependence of ΔH°, ΔG° and $-T\Delta S^\circ$ for the ABC⇆A+BC transition. The triplex concentration was 4.4×10^{-4} M.

4. Discussion

In this work a combination of optical and calorimetric techniques was used to characterize the thermodynamic of triplex formation at different pH values. The DSC experiments clearly show that the thermodynamic parameters associated with triplex dissociation considerably change on varying the pH (Table 1). To explain these data, a thermodynamic model was developed. This model links the cytosine ionization equilibrium to the dissociation process of the triplex. In this effort, the deprotonation constants for the cytosine residues in the free third strand (K_a^S) and inside the triplex structure (K_a^T) were evaluated. The

pK_a^S value for the cytosine residues was obtained by UV titration experiment on the isolated third stand. The value of 4.5, obtained by the inflection point of the titration curve (Fig. 4) is similar to the pK_a value of the free nucleotide indicating that in the free third strand the cytosine residues are exposed to the solvent. It is known that pK_a^T value is generally greater than pK_a^S value due to the local environment of the cytosine residue inside the triplex structure [12–15]. Hence, on increasing the pH, the global dissociation equilibrium will be shifted toward the free third strand by mass action effects. This is consistent with the observed variations of the ellipticity at 215 nm and 5 °C on increasing the pH, shown in Fig. 3. The inflection point of the curve represents the apparent pK_a of the pH-induced transition relative to dissociation of the third strand from the target double helix. However, this value cannot be considered the pK_a^T value because the method evaluates the influence of pH on the global equilibrium process and protonation/deprotonation of individual cytosines within the triplex structure are not directly resolved. A rigorous thermodynamic method to determine the intrinsic pK_a of cytosine residues, was adopted by Wilson et al. They calculated an intrinsic pK_a between 7 and 7.5 for cytosine residues in the same local environment studied by us using binding enthalpy vs. buffer ionization enthalpy data. pK_a^T values in the range suggested by Wilson et al. were used to reproduced experimental data. The best agreement between the experimental and the calculated data was obtained for pK_a^T=7.0 (Fig. 5). The model reveals that the contributions made by the shifts of the coupled deprotonation equilibrium to the observed entropy and enthalpy changes may be significant. Further, although the enthalpic and entropic contributions are both influenced by pH, analysis of the Eqs. (4) and (5) demonstrates that the effect of pH on triplex stability is entropic in origin because at each pH the enthalpy change is exactly compensated by the third term on the right-hand side of Eq. (5). This is a remarkable result that cannot be deduced from a simple inspection of Table 1. Furthermore, it can be noted that the observable of DSC experiments, related to enthalpy change, is strongly dependent on the degree of protonation of the third strand. Indeed, in the spectroscopic experiments, it is possible to measure only the sums of the concentrations of the different protonated species because the protonation does not make a very large difference to the observable. This could be a possible source for the discrepancy between van't Hoff enthalpies obtained by spectroscopic methods and the calorimetric enthalpies, as reported by many authors [26,31,32].

In conclusion, the present model gains more insight into the effect of protonation on the free energy, entropy and enthalpy changes associated with the third strand binding to the target duplex. It was shown in a qualitative and quantitative manner, how the pH influences these thermodynamic parameters for the triplex dissociation. These results could be useful to systematically introduce the effect of pH in a more general model able to predict the stability of DNA triplexes on the basis of the sequence alone.

Acknowledgements

This work was supported by a PRIN-MURST grant from the Italian Ministry and University and Scientific and Technological Research (Rome).

References

[1] V.N. Potaman, Application of triple-stranded nucleic acid structures to DNA purification, detection and analysis, Expert Rev. Mol. Diagn. 3 (2003) 481–496.
[2] R.V. Guntaka, B.R. Varma, K.T. Weber, Triplex-forming oligonucleotides as modulators of gene expression, Int. J. Biochem. Cell. Biol. 35 (2003) 22–31.
[3] M. Faria, C. Giovannangeli, Triplex-forming molecules: from concepts to applications, J. Gene Med. 3 (2001) 299–310.
[4] G. Felsenfeld, D.R. Davies, A. Rich, Formation of three-stranded polynucleotide molecule, J. Am. Chem. Soc. 79 (1957) 2023–2024.
[5] K. Hoogsteen, The structure of crystals containing a hydrogen-bonded complex of 1-methylthymine and 9-methyladenine, Acta Crystallogr. 12 (1959) 822–823.
[6] K. Liu, V. Sasisekharan, H.T. Miles, Structure of Py Pu Py DNA triple helices. Fourier transforms of fiber-type X-ray diffraction of single crystals, G. Raghunathan, Biopolymers 39 (1996) 573–589.
[7] P.A. Beal, P.B. Dervan, Second structural motif for recognition of DNA by oligonucleotide-directed triple-helix formation, Science 251 (1991) 1360–1363.
[8] L. Lavelle, J.R. Fresco, UV spectroscopic identification and thermodynamic analysis of protonated third strand deoxycytidine residues at neutrality in triplex $d(C^+\text{-}T)_6$: $[d(A\text{-}G)_6.d(C\text{-}T)_6]$; evidence for a proton switch, Nucleic Acids Res. 23 (1995) 2692–2705.

[9] G.E. Plum, K.J. Breslauer, Thermodynamics of an intramolecular DNA triple helix: a calorimetric and spectroscopic study of the pH and salt dependence of thermally induced structural transitions, J. Mol. Biol. 248 (1995) 679–695.
[10] J.P. Bartley, T. Brown, A.N. Lane, Solution conformation of an intramolecular DNA triplex containing a non-nucleotide linker: comparison with the DNA duplex, Biochemistry 36 (1997) 14 502–14 511.
[11] N. Sugimoto, P. Wu, H. Hara, Y. Kawamoto, pH and cation effects on the properties of parallel pyrimidine motif DNA triplexes, Biochemistry 40 (2001) 9396–9405.
[12] J.L. Asensio, A.N. Lane, J. Dhesi, S. Bergquist, T. Brown, The contribution of cytosine protonation to the stability of a parallel DNA triple helices, J. Mol. Biol. 275 (1998) 811–822.
[13] L.E. Xodo, G. Manzini, F. Quadrifoglio, G.A. van der Marel, J.H. van Boom, Effect of 5-methylcytosine on the stability of triple-stranded DNA a thermodynamic study, Nucleic Acids Res. 19 (1991) 5625–5631.
[14] D. Leitner, W. Schröder, K. Weisz, Direct monitoring of cytosine protonation in an intramolecular DNA triple helix, J. Am. Chem. Soc. 120 (1998) 7123–7124.
[15] D. Leitner, W. Schröder, K.J. Weisz, Influence of sequence-dependent cytosine protonation and methylation on DNA triplex stability, Biochemistry 39 (2000) 5886–5892.
[16] M. Gait (Ed.), Oligonucleotide Synthesis: A Practical Approach, IRL Press, Oxford, UK, 1984.
[17] F. Eckstein (Ed.), Oligonucleotides and Analogues: A Practical Approach, IRL Press, Oxford, UK, 1991.
[18] L. Petraccone, E. Erra, A. Messere, D. Montesarchio, G. Piccialli, G. Barone, et al., Physico-chemical studies of a DNA triplex containing a new ferrocenemethyl-thymidine residue in the third strand, Biophys. Chem. 104 (2003) 259–270.
[19] C.R. Cantor, M.M. Warshaw, H. Shapiro, Oligonicleotide interactions. Circular dichroism studies of the conformation of deoxyoligonucleotides, Biopolymers 9 (1970) 1059–1077.
[20] G. Barone, P. Del Vecchio, D. Fessas, C. Giancola, G. Graziano, Theseus: a new software package for the handling and analysis of thermal denaturation data of biological macromolecules, J. Therm. Anal. 39 (1993) 2779–2790.
[21] E. Freire, R.L. Biltonen, Thermodynamics of transfer ribonucleic acids: the effect of sodium on the thermal unfolding of yeast tRNAPhe, Biopolymers 17 (1978) 1257–1272.
[22] C. Giancola, A. Buono, G. Barone, L. De Napoli, D. Montesarchio, D. Palomba, et al., J. Therm. Anal. 38 (1999) 1177–1184.
[23] H.P. Hopkins, D.D. Hamilton, W.D. Wilson, Duplex and triple helix formation with dA19 and dT19: thermodynamic parameters from calorimetric, NMR and circular dichroism studies, G. Zon, J. Phys.Chem. 97 (1993) 6555–6563.
[24] R.C. Cantor, P.R. Schimmel, Biophysical Chemistry, Freeman W.H. and Company, San Francisco (USA), 1971, pp. 1145–1147.
[25] V.P. Antao, D.M. Gray, R.L. Ratliff, CD of six different conformational rearrangements of poly[d(A-G).d(C-T)] induced by low pH, Nucleic Acid Res. 16 (1988) 719–738.
[26] G. Manzini, L.E. Xodo, D. Gasparotto, F. Quadrifoglio, G.A. van der Marel, J.H. van Boom, Triple helix formation by oligopurine-oligopyrimidine DNA fragments: electrophoretic and thermodynamic behavior, J. Mol. Biol. 213 (1990) 833–843.
[27] W.D. Wilson, H.P. Hopkins, S. Mizan, D.D. Hamilton, G. Zon, Thermodynamics of DNA triplex formation in oligomers with and without cytosine bases: influence of buffer species, pH and sequence, J. Am. Chem. Soc. 116 (1994) 3607–3608.
[28] G.D. Fasmann, in: CRC Handbook of Biochemistry and Molecular Biology 1,CRC Press Inc, Cleveland, OH, 1975, p. 191.
[29] H. Klump, T. Ackermann, Experimental thermodynamics of the helix-random coil transition IV. Influence of the base composition of DNA on the transition enthalpy, Biopolymers 10 (1971) 513–522.
[30] A.N. Soto, J. Loo, L.A. Marky, Energetic contributions for the formation of TAT/TAT, TAT/CGC^+ and CGC^+/CGC^+ base triplet stacks, J. Am. Chem. Soc. 124 (2002) 14 355–14 363.
[31] J. Völher, D.P. Botes, G.G. Lindsey, H.H. Klump, Energetics of a stable intramolecular DNA triple helix formation, J. Mol. Biol. 230 (1993) 1278–1290.
[32] G.E. Plum, Y.W. Park, S.F. Singleton, P.B. Dervan, K.J. Breslauer, Thermodynamic characterization of the stability and the melting behavior of a DNA triplex: a spectroscopic and calorimetric study, Proc. Natl. Acad. Sci. USA 87 (1990) 9436–9440.